Journal of Non-Crystalline Solids 63 (1984) 45–59
North-Holland, Amsterdam

*Part II. Basic investigations on hydrolysis, condensation and densification II*

# SOL–GEL TRANSITION IN SIMPLE SILICATES II *

C.J. BRINKER, K.D. KEEFER, D.W. SCHAEFER, R.A. ASSINK,
B.D. KAY and C.S. ASHLEY

*Sandia National Laboratories* †, *Albuquerque, New Mexico 87185, USA*

Silica gels were prepared from alcoholic solutions of tetraethylorthosilicate (TEOS) using a two-step hydrolysis process; small angle X-ray scattering (SAXS), gas–liquid chromatography, and $^1$H NMR spectroscopy were employed to study their formation. The first step (1 mol. $H_2O$/mol. TEOS with HCl catalyst) resulted in a rather wide species distribution comprised of hydrolyzed and unhydrolyzed monomers, dimers, and chains. The second step (additional water plus acid or base) resulted in completely hydrolyzed polymers in the acid system which apparently were highly overlapped prior to gelation. In the base system, hydrolysis was incomplete due to unhydrolyzed monomer and the resulting polymers were more highly condensed (or collapsed) and discrete compared to the acid system. The formation of colloidal silica was not observed in either case.

## 1. Introduction

In a previous paper [1] we reported on polymer growth during acid and base catalyzed hydrolysis of tetraethylorthosilicate (TEOS) in alcoholic solutions and proposed that the form of the resulting polymers was governed by the relative rates of hydrolysis and condensation. Under conditions in which condensation is rapid compared to hydrolysis, polysiloxane chains or rings result while in the reverse case more extensively crosslinked polymeric clusters are formed. We have continued our investigations of the hydrolysis and gelation of these solutions using the techniques of small angle X-ray scattering (SAXS), $^1$H NMR, and gas–liquid chromatography (GC) solution analyses. This paper reports on the results of these investigations and in some cases provides a new interpretation of our previous results.

## 2. Experimental

### 2.1. Sample preparation

A two-step process carried out at 25°C (or 60°C SAXS experiments) was used to prepare all the solutions. In the first step TEOS, alcohol (*n*-propanol or

---

* This work performed at Sandia National Laboratories supported by the U.S. Department of Energy under contract no. DE-AC04-76-DP00789.

† A US DOE facility.

0022-3093/84/$03.00 © Elsevier Science Publishers B.V.
(North-Holland Physics Publishing Division)

Table 1

Compositions investigated (mol.%)

*Initial hydrolysis*

| Sample | Solvent'[a] | $H_2O$ | TEOS | HCl | Final pH |
|---|---|---|---|---|---|
| A2, B2 | 59.4 | 21.0 | 19.6 | 0.015 | 0.30 |
| A3, B2 (NMR) | 65.4 | 17.9 | 16.7 | 0.012 | – |

*Final hydrolysis*

| Sample | Solvent[a] | $H_2O$ | TEOS | HCl | $NH_4OH$ | $H_2O$/TEOS | Final pH |
|---|---|---|---|---|---|---|---|
| A2 | 32.8 | 55.7 | 10.9 | 0.632 | – | 5.1 | 0.95 |
| A3 (NMR) | 22.7 | 71.6 | 5.8 | 0.004 | – | 12.4 | – |
| B2 | 39.2 | 47.9 | 12.9 | 0.010 | 0.016 | 3.7 | 7.80 |
| B2 (NMR) | 45.5 | 42.9 | 11.6 | 0.009 | 0.014 | 3.7 | – |

[a] Solvent was *n*-propanol for all samples except NMR where ethanol was the solvent.

ethanol), $H_2O$ and HCl were mixed in the approximate molar ratio 1 : 3 : 1 : 0.0007. This amount of water is one-half that required to form anhydrous silica according to the net reaction

$$Si(OR)_4 + 2H_2O \rightarrow SiO_2 + 4ROH. \tag{1}$$

After 90 min of mixing additional water plus acid (HCl) or base ($NH_4OH$) were added comprising the second step. The specific compositions investigated are listed in table 1.

The hydrolyzed solutions were maintained at 25°C (or 50°C SAXS experiments) until gelled. During the course of hydrolysis and gelation, aliquots of solution were extracted and cooled to −78°C (dry ice + ethanol) to quench the reaction. One set of samples used in the SAXS experiments was diluted by a factor of ten with solvent prior to cooling.

### 2.2. Small angle X-ray scattering

The small angle X-ray data were obtained using the 10M SAXS system at the National Center for Small Angle Scattering Studies associated with the Oak Ridge National Laboratory. All data were taken at the highest resolution (5 m sample to detector distance) using an X-ray source power of about 2 kW and incident beam wavelength of 1.54 Å (CuK$\alpha$). Run times of 2 to 10 min provided adequate signal-to-noise ratios. Solutions sampled during the course of gelation were injected into stainless steel sample cells with 0.025 mm thick MYLAR windows and 1 mm path lengths. The cells were supported in a thermostated block maintained at less than 10°C.

### 2.3 Gas chromatography

Gas–liquid chromatography (GC) was used to monitor hydrolysis and polymerization during gelation in a manner similar to that of Peace et al. [2].

Solutions were prepared as described in §2.1 except 4 vol.% acetone was added to the solution during the first hydrolysis as an internal standard. 0.01–0.02 $\mu$l of the extracted solutions were injected into a 1.8 m × 0.32 cm TENAX (80–100 mesh) filled glass column. A thermal conductivity detector combined with a CDS 111 integrator were used to monitor the volume ratios of EtOH, *n*-PrOH, and $H_2O$, to acetone during the course of gelation. Molar concentrations of EtOH, *n*-PrOH, and water were determined from calibration curves made from unreacted mixtures of the starting compounds.

### 2.4. $^1H$ NMR

$^1$H nuclear magnetic resonance spectra were recorded at 360 MHz on a Nicolet spectrometer at the Colorado State University NSF Regional NMR Facility. All spectra were recorded at room temperature using 4 pulses at a 2 s repetition rate. The samples were run undiluted because a reference solvent may have influenced the reaction kinetics. All resonances were referenced to tetramethylsilane via the ethanol methylene group whose chemical shift is reported as 3.70 ppm relative to tetramethylsilane [3].

## 3. Results and discussion

### 3.1. SAXS results

Small angle X-ray scattering (SAXS) was used to determine the size and growth kinetics of polymeric species formed prior to gelation (by analysis of the low angle, Guinier, region) and to obtain information about the structure of these species (by analysis of the intermediate angle, Porod, region). Scattering in the Guinier region depends on the characteristic dimension, $R$, of the scattering entities and that in the high angle, Bragg, region is governed by short range chemical structures of typical dimension, $a$, e.g. the monomer size. In contrast, scattering in the Porod region, defined as $KR \gg 1 \gg Ka$ where $K$ is related to the scattering angle, $\theta$, by

$$K = (4\pi/\lambda)(\sin\theta/2), \tag{2}$$

depends on the geometric structure of the scattering entities. For example, in a log–log plot of scattered intensity versus the scattering vector, $K$, the slope in the intermediate region is predicted to equal $-2$ for a random walk polymer chain or a randomly branched chain [4], and $-4$ for a particle with sharp (well defined) boundaries [5]. This power law behavior is universal, i.e., it is independent of both the size and the short range chemical details of the scattering entities.

If silica polymerization produces colloidal particles, a $K^{-4}$ power law is predicted [5]. The lower curves of fig. 1 show a $K^{-4}$ power dependence for two known colloidal systems: LUDOX HS40, a colloidal silica, and ferrofluid, a

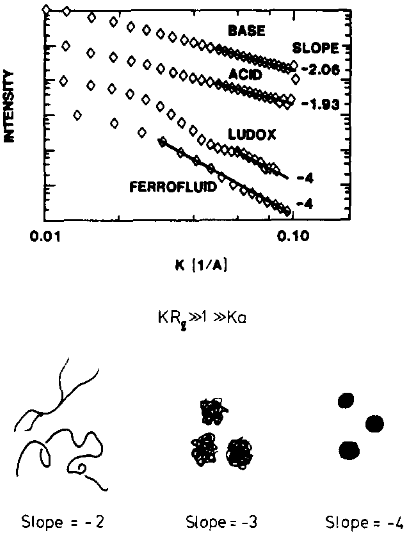

Fig. 1. SAXS profiles of base (B2) and acid (A2) prepared solutions near their respective gel points compared to colloidal sols. In the Porod region the scattered intensity is proportional to $K^{-x}$. Slope analyses differentiate between linear or randomly branched chains, $x = 2$, and colloidal particles, $x = 4$.

dispersion of colloidal magnetite. The scattering curves obtained for acid and base catalyzed silica solutions are shown in the upper part of fig. 1. These solutions were extracted near the respective gel points and diluted 10 : 1 prior to quenching. During polymerization both systems show a Porod slope near $-2$. Such a slope is indicative of an open random polymer molecule with no distinct surface. A Porod slope of $-2$ is expected for ideal linear polymers as well as structures arising from a random bond percolation process [4]. By contrast kinetic [6] and diffusion-limited growth [7] give $-2.5$ and swollen linear chains [8] yield a slope between $-1.66$ and $-2$. In the acid-catalyzed case, Porod slopes are consistently (throughout the course of the second hydrolysis) more positive than $-2$, while for the base-catalyzed system, Porod slopes are consistently more negative than $-2$. Although deviations from $-2$ were not great in either case, deviations toward slopes more positive than $-2$ indicate a crossover between branched and swollen linear chains. This suggests that the acid-catalyzed molecules are so slightly branched that the distance between branches is comparable to $K^{-1}$ ($\sim 20$ Å). An exponent of $-2$ is expected if the system fell in the percolation universality class. Deviations toward more negative slopes suggest that either the base-catalyzed molecules are more highly branched so that crossover toward dense structures (slope = $-4$) is observed or that base-catalyzed molecules are collapsed relative to ideal random linear polymers.

The low angle Guinier region was analyzed to determine the apparent radius of gyration, $R_g$. In our initial paper [1] we found that for acid-catalyzed

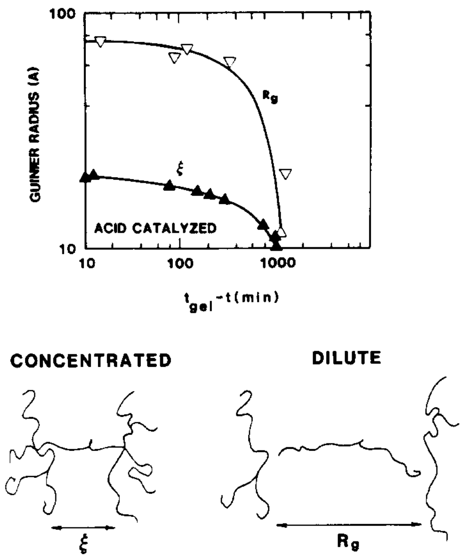

Fig. 2. Guinier radius as a function of time-to-gelation for A2. The correlation range, $\xi$, is measured on undiluted (concentrated) samples while the radius of gyration, $R_g$, is measured on diluted samples.

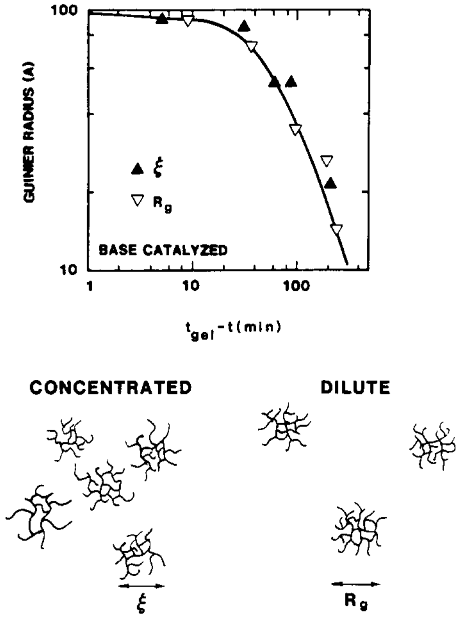

Fig. 3. Guinier radius as a function of time-to-gelation for B2.

systems (e.g. A2) the low angle portion of the scattering curves did not change during the second hydrolysis and subsequent gelation suggesting that the size and shape of the silicate molecules did not vary. In contrast, the scattering curve of the base-catalyzed sample, B2, changed considerably during the course of gelation. The apparent radius of gyration grew from 20 Å, 1.2 h after the addition of the base, to 44 Å after 3.8 h during which time gelation occurred. This interpretation, however, was based on the assumption that we were measuring a dimension ($R_G$) which was truly representative of the size of the molecule and unaffected by intermolecular correlations.

To test this hypothesis, the above experiment was repeated using both diluted and undiluted samples. In the diluted samples where we assume the molecules do not interpenetrate, $R_G$ is the radius of gyration, $R_g$, of the molecules. If interpenetration does occur as might be expected in the undiluted case, the apparent $R_G$ is equal to the correlation range, $\xi$. If the molecules are overlapped and entangled prior to gelation, then $\xi$ is concentration-dependent [9] and substantially smaller than $R_g$. Conversely, if the solution is sufficiently dilute so that no overlap occurs prior to gelation, $\xi$ is concentration-independent and equivalent to $R_g$.

Figs. 2 and 3 show the measured $R_G$ as a function of time-to-gelation ($T_{gel}$-$T$). Except near the start of the reaction, $R_G$ is considerably larger than $\xi$ for the acid-catalyzed system (fig. 2). This discrepancy implies that for all later stages of reaction the silicate molecules are strongly overlapped in the undiluted (semidilute [9]) solution. $R_G$ is concentration-independent in the base-catalyzed system (fig. 3). This implies that these molecules must be sufficiently dilute (separated) so that little overlap occurs prior to gelation.

Because for equivalent initial concentrations of monomer and equivalent amounts of polymerization, chains are more likely to overlap than highly-branched entities, these results suggest that the polymers formed in the acid-catalyzed solutions are extended, weakly-branched chains whereas polymers formed in base-catalyzed solutions are discrete, more highly-branched clusters. This interpretation is consistent with our analyses of intermediate angle scattering and explains why in our previous investigation we saw little apparent growth of the molecules in the acid-catalyzed system.

### 3.2. GC solution analyses

The hydrolysis reaction produces ethanol and consumes water, and the condensation reaction releases water (and possibly ethanol). Thus, the course of these reactions may be monitored by GC analyses for EtOH and $H_2O$. Normal propanol was used as a solvent to improve the accuracy of the ethanol analysis. Ester exchange was determined by simultaneously measuring the amount of solvent consumed which must be equal to the amount of ethanol liberated by the exchange process. Our results are shown in figs. 4 and 5 which plot the average number of OEt, OH, OSi and OPr (bonded to Si) per Si atom as a function of reaction time.

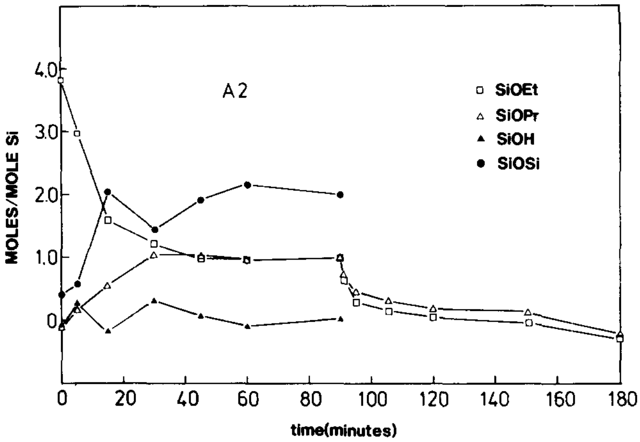

Fig. 4. Results of GC solution analyses for A2 showing the average molar concentrations of silicon species as a function of reaction time. Due to inconsistent analyses for $H_2O$ in the second stage of hydrolysis SiOH and SiOSi are plotted for the initial stage of hydrolysis only (0–90 min).

The initial hydrolysis (0–90 min) was carried out using 1 mol. of $H_2O$/mol. TEOS with HCl as the catalyst. The important features of this stage are: (1) hydrolysis and condensation occur rapidly as evidenced from the reduction of alkoxy groups on silicon and from the absence of a significant amount of OH groups; (2) ester exchange is substantial as the ratio of SiOPr to SiOEt increases from zero to nearly unity in ~ 60 min; (3) on the average approximately 2 SiOSi bridges per silicon atom have formed after 90 min. These results suggest that the reaction has gone to completion by the end of the first hydrolysis step.

At the start of the second hydrolysis (90 min of reaction time) additional

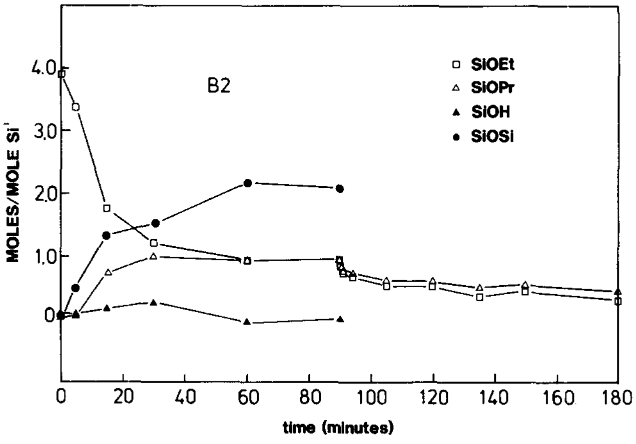

Fig. 5. Results of GC solution analyses for B2.

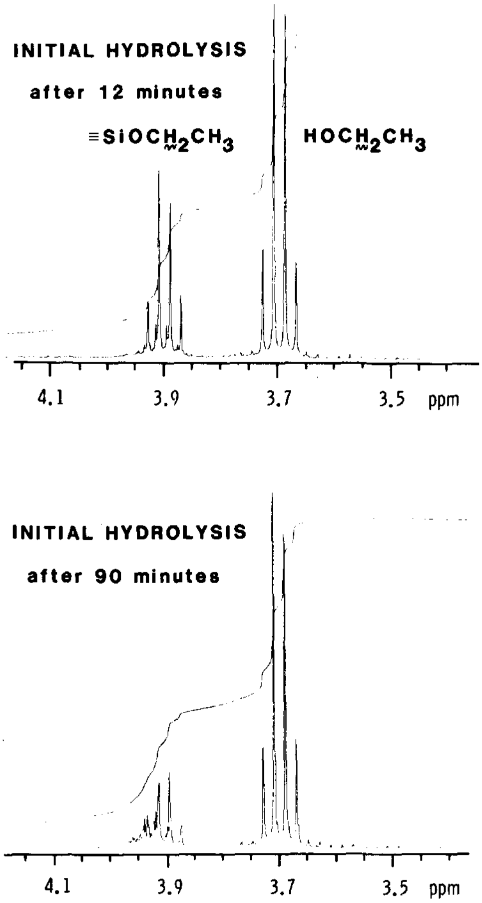

Fig. 6. $^1$H NMR spectrum taken during the initial hydrolysis (a) after 12 min of reaction, (b) after 90 min.

water plus acid (A2) or base (B2) were added to the reacted solution. In the acid case, complete hydrolysis of the OEt and OPr side groups occurs within 60 min of this addition. In the base system, hydrolysis appears to proceed more slowly. In fact, the system gels (3.5 h of reaction time) before hydrolysis is complete. For both the acid and base systems, the hydrolysis of OEt and OPr closely parallel each other during the second hydrolysis step; the rate of hydrolysis of OEt being slightly greater than that of OPr as is expected from both steric and inductive effects.

### *3.3. Proton NMR results*

$^1$H nuclear magnetic resonance spectra were recorded to more sensitively monitor the hydrolysis reactions and to determine the speciation of silicon during the course of gelation. For these experiments, ethanol was used as the solvent to eliminate transesterification and to simplify the spectral interpretation.

Figs. 6a and b show an expansion of the 3.5 to 4.1 ppm spectral region for short and long times during the initial hydrolysis. The quartet centered at 3.90 ppm is the resonance of the methylene protons associated with TEOS and is most sensitive to changes occurring around the silicon to which it is attached. The quartet centered at 3.70 ppm is the resonance of the methylene protons of ethanol. Two qualitative changes occur with time. First, the quartet at 3.90 ppm is becoming a more complex superposition of many quartets as the functional groups about the attached silicon become more varied [for more

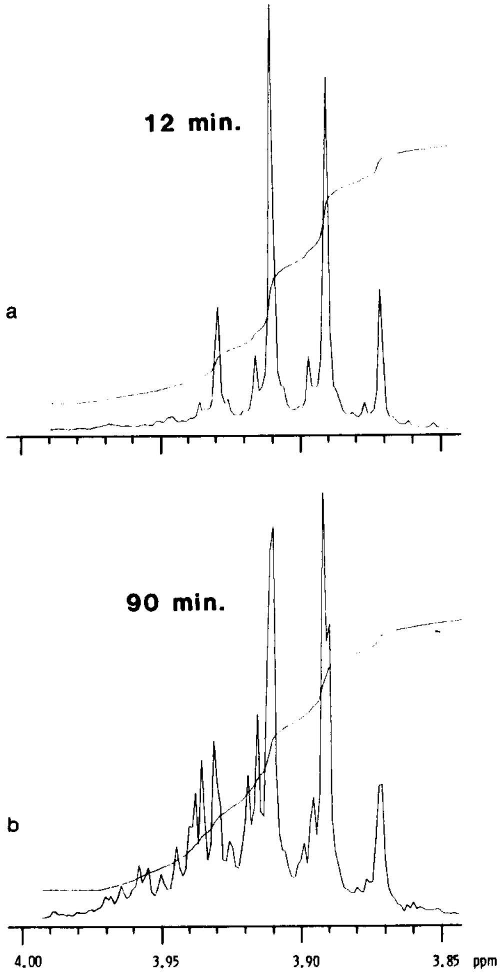

Fig. 7. $^1H$ NMR multiplet centered at 3.90 ppm (a) after 12 min of the initial hydrolysis, (b) after 90 min of the initial hydrolysis.

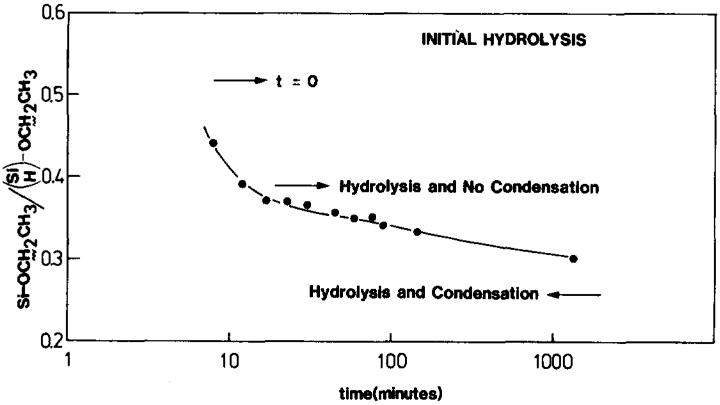

Fig. 8. Methylene groups on silicon per total methylene groups during the initial hydrolysis. Arrows indicate the theoretical values corresponding to ($t = 0$), hydrolysis and no condensation, and hydrolysis and condensation.

detail see figs. 7a and 7b]. Second, the intensity of the methylene quartet associated with a silicon is decreasing relative to the quartet associated with ethanol as hydrolysis proceeds. This effect is easy to quantify by integrating the appropriate peaks centered at 3.70 and 3.90 ppm respectively and will be used here to determine the extent of hydrolysis.

Fig. 8 shows the fraction of methylene groups associated with a silicon relative to the total number of methylene groups during the first hydrolysis. Also shown are arrows corresponding to the theoretical initial and final values assuming, (i) complete hydrolysis but no condensation, and (ii) complete hydrolysis plus condensation. The results show that the value corrresponding to complete hydrolysis is attained in the first 12 min, and the value corresponding to hydrolysis plus condensation is approached during the initial stage. This is consistent with the GC results. The $^1H$ NMR results show, however, that the reaction is not complete after 90 min. This apparent inconsistency may reflect the increased sensitivity of this technique or may result from subtle differences in preparative methods or the change in solvent.

Separation of the 3.90 ppm region into its various components can yield detailed chemical information concerning the local polymer structure, i.e. it is possible to determine the fifth nearest neighbors of methylene protons associated with silicon: either hydrogen ($\equiv$ Si–OH), carbon ($\equiv$ Si–OEt), or silicon ($\equiv$ Si–OSi). In theory, it is possible to identify 10 different silicon species representing various hydrolyzed forms of monomers, dimers, chains, and sheets. Only fully hydrolyzed or fully condensed species are undetected by this analysis.

A quantitative deconvolution of this region will not be attempted in the present paper; however, we can qualitatively state that, during approximately the first 12 min of the initial hydrolysis, singly, doubly, and possibly triply

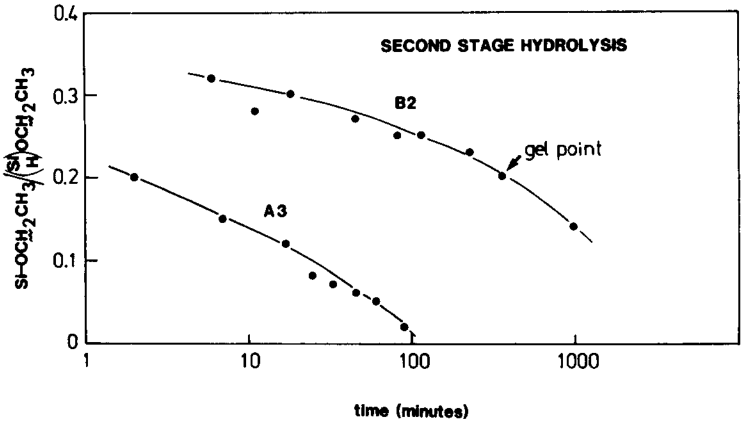

Fig. 9. Methylene groups on silicon per total methylene groups during the second stage hydrolysis for A3 and B2.

hydrolyzed monomers are formed which subsequently condense and hydrolyze to form primarily dimers after 90 minutes and dimers plus chainlike (or cyclic) structures after 24 h. Unhydrolyzed monomer is detected throughout the course of this initial stage.

The time dependence of hydrolysis during the second step is shown in fig. 9. Again consistent with the GC analyses, the results indicate that the extent of hydrolysis is greater in the acidic system than in the basic system which gels before it is completely hydrolyzed.

## Discussion

### 4.1. First hydrolysis step

The combined results presented here can be used to illustrate the important aspects of polymer growth prior to gelation. The first hydrolysis is conducted with an acid catalyst and 1 mol. $H_2O$/mol. TEOS. As evidenced by the rapid decrease in Si–OEt [GC results (figs. 4 and 5) and NMR results (fig. 8)], all of the added water is consumed in the first few minutes of reaction to produce predominately a distribution of hydrolyzed monomers. Because more than singly hydrolyzed monomers are formed during this period, it is necessary that corresponding amounts of monomer remain unhydrolyzed in order to maintain stoichiometry. Examination of the 3.90 ppm region of the NMR spectrum shows this to be the case. Whether the specific distribution of monomers which results during the first few minutes of reaction depends more on the amounts of added reagents or on the precise manner of their addition, i.e. degree of mixing and order of addition, cannot be ascertained at present.

During the remainder of the initial hydrolysis step, subsequent condensation and hydrolysis reactions result in the formation of polymers, i.e. dimers and chain-like or cyclic species. GC analyses of systems prepared in *n*-propanol suggest that the reaction represented by the following net equation

$$n\mathrm{Si(OR)_4} + \mathrm{ln}\ \mathrm{H_2O} \rightarrow n\mathrm{SiO(OR)_2} + 2n(\mathrm{ROH}), \qquad (3)$$

is complete after the first 90 min, i.e. all of the water is consumed and the resulting polymers are nearly fully esterified. NMR analyses of systems prepared in ethanol indicate that intermediate species, $\mathrm{SiO}_x\mathrm{OH}_y\mathrm{OR}_z$ (where $2x + y + z = 4$), are present after 90 min and that the reaction approaches completion only after 24 h. In either case, there is no NMR or SAXS evidence that the distribution of polymers represented by the stoichiometry, $\mathrm{SiO(OR)_2}$, consists of $\frac{1}{2}\mathrm{SiO_2} + \frac{1}{2}\mathrm{Si(OR)_4}$, i.e. the solution does not contain monomer plus colloidal silica after the first 90 min of reaction.

Colloid formation (even with the addition of only 1 mol. $\mathrm{H_2O}$/mol. of TEOS) is expected when hydrolysis is rapid compared to condensation and each successive hydrolysis reaction occurs more readily than the previous one (as, for example, in a nucleophilic hydrolysis reaction). If this were the case, orthosilicic acid monomers would subsequently condense according to:

$$\equiv \mathrm{SiO^-} + \mathrm{HOSi} \equiv \; \rightarrow \; \equiv \mathrm{SiOSi} + \mathrm{OH^-} \qquad (4)$$

the nucleophilic attack of a deprotonated silanol on a protonated one. Because the most highly condensed silanol species are also the most acidic (and conversely the least highly condensed the least acidic), this reaction tends to form highly condensed and crosslinked species of colloidal dimension [10]. Therefore according to this reaction sequence, the addition of 1 mol. $\mathrm{H_2O}$/mol. TEOS could ultimately result in $\frac{1}{2}$ mol. of colloidal silica plus $\frac{1}{2}$ mol. of unhydrolyzed monomer. Although there is qualitative evidence for colloid formation in the base catalyzed hydrolyses of TEOS [11], both the SAXS and NMR results show no indication of colloid formation during the initial hydrolysis step. Thus in acid catalyzed solutions of TEOS prepared with insufficient water, monomeric silanol species start to condense before they are fully hydrolyzed leading to the formation of dimers and chain-like structures rather than colloidal particles.

The concepts developed here to explain the initial hydrolysis reaction are in qualitative agreement with the findings of Sakka and Kamiya [12]. They reported that aged solutions prepared with 1 mol. $\mathrm{H_2O}$/mol. TEOS and HCl as a catalyst were spinnable and exhibited a strong concentration dependence on reduced viscosity: further evidence for linear polymers.

### 4.2. Second hydrolysis step

The second reaction step is the acid (A2,3) or base (B2) catalyzed hydrolysis of a distribution of oligomeric and monomeric species of small ($R_g < 10$Å) dimensions. Interestingly, both the GC and NMR analyses show that the second stage base-catalyzed hydrolysis is incomplete, whereas the second stage acid-catalyzed hydrolysis quickly goes to completion. This result was also reported by Yamane et al. for acid- and base-catalyzed hydrolysis of silicon methoxide [13]. Deconvolution of the superimposed multiplets centered at ~ 3.90 ppm (e.g. fig. 7) shows that, for the base-catalyzed case, the intensity of peaks associated with chains, dimers, and hydrolyzed monomers (except perhaps singly hydrolyzed monomers) diminishes quickly with time during the second hydrolysis step as hydrolysis and condensation proceed, ultimately resulting in complete hydrolysis and/or condensation. However, the intensity of the quartet associated with the unhydrolyzed monomer (TEOS) and possibly the singly hydrolyzed monomer changes very little throughout the course of this hydrolysis step. This suggests that all the added water and catalyst are preferentially associated with the various hydrolyzed and condensed species consistent with a phase separation process.

By contrast, in the acid-catalyzed system, A3, the intensities of all the peaks comprising the superimposed 3.90 ppm multiplets diminish at comparable rates during the second hydrolysis step. Thus, there appears to be no chemical evidence of phase separation in the acid-catalyzed system.

The differences in polymer topology which occur during the second hydrolysis step, i.e. extended chains (A2) versus more highly branched clusters (B2) may be explained by the pH dependences of solubility, condensation and perhaps phase separation. First, because the solubility of siloxane networks is roughly proportional to $OH^-$ concentration, depolymerization is expected for B2 (pH ~ 8) [10]. Therefore, in the base system, polymers formed in the first hydrolysis step dissolve and repolymerize in a more highly condensed form; whereas in the acid system the original polymer configuration is preserved (i.e., polymerization is essentially irreversible in acid systems).

Second, if during the second hydrolysis step polymerization occurs by a nucleophilic reaction [eq. (4)], condensation should occur preferentially between protonated and deprotonated silanols. In the base catalyzed system, middle groups on chains are more acidic than end groups on chains. Therefore, condensation reactions are likely to occur between ends and middles of chains promoting the formation of more highly condensed clusters. Because some dissolution of the polymers occurs concurrently, and at the start of the second hydrolysis step a distribution of smaller polymers is observed, ripening of these clusters will also occur. Finally, the increased pH in B2 appears to have caused phase separation. If so, large fluctuations in polymer density result. Those regions containing more highly hydrolyzed and condensed species coagulate leaving solvent rich regions containing unhydrolyzed monomer.

Thus, there are several mechanisms by which the base catalyzed system might result in cluster formation. It is important to emphasize, however, that none of these mechanisms (condensation, ripening, or phase separation) result in the formation of colloidal particles under the conditions studied. Apparently, the pH is not sufficiently high to completely restructure the original polymer configuration.

The acid-catalyzed system is less well understood. GC results indicate that hydrolysis is complete after ~ 60 min of the second step long before the system gels (> 1000 min). Polymer growth observed throughout this hydrolysis step (fig. 2) results in extended linear or randomly branched polymers, i.e. the distance between branches is > 20 Å. According to Aelion et al., under acid conditions, dimers or end groups on chains are more readily hydrolyzed than middle groups on chains [14]. Therefore at the beginning of the second hydrolysis step, it is expected that hydrolysis reactions are directed toward the ends of polymers formed during the initial step. Subsequent condensation reactions [according to eq. (4)] are therefore initially more likely to occur between ends of chains resulting in primarily linear polymers. Complete hydrolysis (after 60 min) results in a system comprised of fully hydrolyzed linear and/or randomly branched chains. Because under acid conditions ($pH < 2.5$) most silanols are protonated, the rate of condensation according to eq. (4) is slow. Thus, these polymers can entangle but because they are highly protonated, do not readily condense to form a gel. Under acid conditions, therefore, the structure of the polymers results primarily from the distribution of silanols produced during the hydrolysis reactions and not from the condensation process.

Finally, it should be noted that in our initial report [1] we concluded that acid-catalyzed hydrolysis (as, e.g., in A2) should result in small, incompletely hydrolyzed, weakly branched polymers. This conclusion was based on the results of pyrolysis experiments which showed that gel A2, when desiccated, contained 0.22 EtO/Si. This apparent inconsistency with our present results, which show complete hydrolysis, indicates that during desiccation extensive re-esterification can occur for acid catalyzed systems prepared with relatively low water contents. This is consistent with models proposed by Keefer [15] for acid and base catalyzed hydrolysis and esterification of polysilicates.

## 5. Conclusions

From this phase of the investigation we conclude that neither the acid- or the base-catalyzed conditions employed here resulted in the formation of colloidal silica. Instead extended linear or randomly branched polymers were formed under acid conditions which were highly overlapped prior to gelation. The base-catalyzed system resulted in discrete and perhaps more highly condensed clusters which remained dilute up to the gel point. The apparent reduction in the overall rate of hydrolysis for base-catalyzed systems may result from phase separation in which unhydrolyzed monomer resides in a solvent rich phase void of water and catalyst.

The authors would like to thank F.B. Burns and P.J. Rodacy for their contributions to the GC analyses. Also the support of the Colorado State University Regional NMR Center, funded by National Science Grant No. CHE-8208821, and the National Center for Small Angle Scattering Studies, affiliated with Oak Ridge National Laboratory, are gratefully acknowledged.

## References

[1] C.J. Brinker, K.D. Keefer, D.W. Schaefer and C.S. Ashley, J. Non-Crystalline Solids 48 (1982) 47.
[2] B.W. Peace, K.G. Mayhan and J.F. Montle, Polymer 14 (1973) 420.
[3] N.S. Bhacca, L.F. Johnson and J.N. Shoolery, NMR Spectra Catalog (Varian Associates, Palo Alto, CA, 1962).
[4] D. Stauffer, A Coniglio and M. Adams, in: Advances in Polymer Science, Vol. 44 (Springer, Berlin, 1982).
[5] G. Porod., Kolloid Z. 124 (1951) 83.
[6] H.J. Herrmann and D.P. Landau, Phys. Rev. Lett. 49 (1982) 412.
[7] T. Witten and L.M. Sander, Phys. Rev. Lett. 47 (1981) 1400.
[8] D.W. Schaefer and J.G. Curro, Ferroelectrics 30 (1980) 49.
[9] D.W. Schaefer, Polymer (1983), to be published.
[10] R.K. Iler, The Chemistry of Silica (Wiley, New York, 1979).
[11] M. Nogami and Y. Moriya, J. Non-Crystalline Solids 37 (1980) 191.
[12] S. Sakka and K. Kamiya, J. Non-Crystalline Solids 48 (1982) 31.
[13] M. Yamane, S. Inoue and A. Yasumori, these Proceedings (Glasses and Glass Ceramics from Gels 2), p. 13.
[14] R. Aelion, A. Loebel and F. Eirich, J. Am. Chem. Soc. 72 (1950) 5705.
[15] K.D. Keefer, presented at 85th Annual Meeting Am. Ceram. Soc., Chicago (1983), to be published.

## Discussion

*Q*. Is an equilibrium reached in the acid-catalyzed hydrolysis reaction?

*A*. It was found that the reaction continues to proceed even after a thousand hours with 1 mol. ratio of $H_2O$/TEOS. It looks like the reaction is approaching an equilibrium in which hydrolysis is not complete.

*Q*. Are the results achieved by $^1H$ NMR consistent with those achieved by $^{29}Si$ NMR?

*A*. At present, the full interpretation of the results obtained by $^{29}Si$ NMR analysis is more difficult than the $^1H$ NMR analysis. But no inconsistencies are obtained between the two.

*Q*. What explanation do you have for the differences between acid- and base-catalyzed processes?

*A*. In the case of hydrolysis, the acid-catalyzed mechanism involves electrophilic attack, while the base mechanism is a nucleophilic one.

*Q*. It is hardly imaginable that in the case of acid catalysis $\equiv Si{-}O^-$ species will play any role in the rate determining step.

*A*. If, in the acid system, the extended polymers are fully protonated and condensation occurs by a nucleophilic process involving $\equiv Si{-}O^-$, condensation to form a gel would be very slow as is observed, However, there may be an alternative mechanism, i.e. an electrophilic condensation mechanism, which is consistent with the observed results.